

Metal Oxide Coated Lithium Cobalt Fluorophosphate Cathode Materials for Lithium Secondary Batteries—Effect of Aging and Temperature

S. Amaresh¹, K. Karthikeyan^{1,2}, K. J. Kim¹, J. Y. An¹, S. J. Cho¹, K. Y. Chung³,
B. W. Cho³, K. W. Nam^{4,5,*}, and Y. S. Lee^{1,*}

¹Faculty of Applied Chemical Engineering, Chonnam National University, Gwangju 500-757, Korea

²Department of Mechanical and Materials Engineering, The University of Western Ontario, London, Ontario, N6A 5B9, Canada

³Center for Energy Convergence, Korea Institute of Science and Technology, Seoul 136-791, Korea

⁴Chemistry Department, Brookhaven National Laboratory, Upton, NY 11973, USA

⁵Department of Energy and Materials Engineering, Dongguk University-Seoul, Seoul, 100-715, Korea

Lithium cobalt fluorophosphate ($\text{Li}_2\text{CoPO}_4\text{F}$) is a promising 5 V class cathode material for lithium secondary batteries. In this study, surface coating with ZrO_2 improved the electrochemical activity of $\text{Li}_2\text{CoPO}_4\text{F}$ with a maximum discharge capacity of 144 mA h g^{-1} . The effectiveness of ZrO_2 coating was evaluated using aging analysis with a commercial electrolyte, i.e., 1 M LiPF_6 in EC:DMC (1:1, v/v). The metal ion dissolution was reduced to 1/8th of that observed in the non-coated $\text{Li}_2\text{CoPO}_4\text{F}$. It was found that the thin coating layer had less or no contribution to the additional resistance for the cell, both at an open circuit potential and at a fully charged state; hence, the capacity of the cell was retained over cycling. Elevated temperature aging did not affect the intrinsic property of the coated $\text{Li}_2\text{CoPO}_4\text{F}$, as observed from the complete anodic and cathodic peaks from cyclic voltammetry studies after 30 days of storage at 50°C . An increase in impedance was observed for aged cells, which could be due to the thick SEI layer formed during storage. The ZrO_2 coating over $\text{Li}_2\text{CoPO}_4\text{F}$ was crucial for the improved performance of electrode active material at higher operating potentials of up to 5.2 V.

Keywords: Aging, Cathode, $\text{Li}_2\text{CoPO}_4\text{F}$, ZrO_2 , Coating, Lithium Battery.

1. INTRODUCTION

Research on cathode materials during the past few decades to realize the performance of lithium secondary batteries has focused mostly on transition metal oxide having the general formula of Li_xMO_2 (where $\text{M} = \text{Co}, \text{Ni}, \text{Mn}$).^{1–6} The metal oxides were based on two-dimensional close-packed oxygen stacking, which was operated by a $\text{M}^{4+}/\text{M}^{3+}$ redox mechanism with easy insertion and extraction of lithium ions due to acceptable ionic and electronic conductivities. These oxides had a tendency to restack during high lithium extraction and proceeded to irreversible structural modification that led to severe capacity loss during cycling.⁷ Three-dimensional oxides such as LiMn_2O_4 were introduced, which had an improved conduction pathway for lithium with an operating voltage as high as 4.2 V

versus Li^+/Li .^{7,8} A similar framework structure based on transition metal and polyanion $(\text{PO}_4)^{3-}$ was proposed by Padhi et al. that had the molecular formula of LiFePO_4 .⁹ Intense research work was focused on polyanion compounds due to their structural stability, in order to exhibit a good long term cycleability and a relatively higher operating voltage.^{10–14} A wide variety of atomic arrangements and crystal structures were obtained for polyanionic compounds with substitutions based on different classes of cations and anions.¹⁵ An extension of these framework structures was provided by the class of fluorophosphates that relied extensively on the stability and inductive effect of polyanions coupled with a highly electronegative fluoride anion which lowered the energy of the given transition metal redox couple. Only four classes of lithium or sodium fluorophosphates have been reported so far in the literature, namely AMPO_4F , $\text{A}_3\text{M}_2(\text{PO}_4)_2\text{F}_3$, $\text{A}_2\text{MPO}_4\text{F}$, and

* Authors to whom correspondence should be addressed.

$\text{A}_5\text{M}(\text{PO}_4)_2\text{F}_2$, where A = Li or Na and M = V, Cr, Mn, Ni, Co, Fe, Al, Ga.^{16–20}

The lithium cobalt fluorophosphate (LCPF), represented by the molecular formula $\text{Li}_2\text{CoPO}_4\text{F}$, was of interest in this study due to the higher operating voltage exhibited by the compound. The structure of $\text{Li}_2\text{CoPO}_4\text{F}$ consisted of CoO_4F_2 octahedra, PO_4 tetrahedra, and LiO_6 octahedra. The crystal structure of $\text{Li}_2\text{CoPO}_4\text{F}$ adopted an orthorhombic symmetry with the *Pnma* space group in a 3D framework network. Infinite chains of CoO_4F_2 formed by edge sharing of the octahedra are aligned along the *b* axis. The 3D framework structure was constructed by linking the octahedral chains with the PO_4 tetrahedra, which delimited the tunnels aligned along the *b* axis where the lithium ions are located. Using bond valence sum (BVS) calculations, Hadermann et al.²⁰ found that the Li (2) and Li (3) atoms at the 4*c* location had nominal valence of +1. In contrast, the Li(1) cation at 8*d* location was under bonded with reduced BVS and hence this site was responsible for lithium extraction. A similar process was observed in the case of the $\text{Li}_2\text{Ni}_{0.75}\text{Fe}_{0.25}\text{PO}_4\text{F}$ compound while extracting lithium ions. It is very difficult to extract lithium ions from an LCPF compound. Khasanova et al.²¹ reported a structural transformation during the initial extraction in $\text{Li}_2\text{CoPO}_4\text{F}$ at 4.8 V which was irreversible, but the insertion/extraction continued with the modified framework formed during the initial charge. In spite of these difficulties, the framework $\text{Li}_2\text{CoPO}_4\text{F}$ could be considered as a promising positive electrode material because of its high theoretical capacity, which is twice that of olivine LiCoPO_4 if two alkali cations are extracted successfully.²²

Various types of coatings have been studied and significant improvement in capacity retention at high operating voltage has been demonstrated, while the ZrO_2 coated sample has exhibited the best results in the case of LiCoO_2 electrode materials.²³ The variation in the *c* axis was suppressed by ZrO_2 coating and was believed to be the main reason behind the effectiveness of capacity retention. It was also proposed that the variation range of the *c* axis during high voltage cycling can be reduced with protective coating, which in turn severely affected the capacity fading mechanism of the active material. A surface coating with oxide based materials was effective in improving the electrochemical performance of the cathode material due to the suppressed side reactions such as decomposition of electrolytes at high voltages. In addition, surface coatings prevented direct contact of the surface of active materials and restrained large volume changes in the lattice during lithium insertion. Moreover, the surface coatings prevented the dissolution of metal ions in active materials during charge/discharge, in reaction with the acidic electrolyte decomposition products.^{23–26}

In our earlier attempt, we successfully demonstrated slightly more than one lithium ion extraction for LCPF, in which a protective coating was utilized at a higher operating voltage.²⁷ The aim of this report is to analyze the

effect of protective coating, i.e., ZrO_2 , in the electrochemical insertion and extraction of LCPF. An aging analysis for determining the effect of protective coating on the metal dissolution was also carried out. The results based on various analyses including cyclic voltammetry, electrochemical impedance spectroscopy, ICP, SEM-EDX, and elemental mapping will be discussed in detail.

2. EXPERIMENTAL DETAILS

$\text{Li}_2\text{CoPO}_4\text{F}$ (LCPF) powders were synthesized by the conventional two step solid state method as reported elsewhere.²⁸ Briefly, the precursor of lithium, cobalt, and phosphate was mixed by ball milling. The first step involved the formation of LiCoPO_4 by firing the precursor at 400 and 800 °C. The second step involved the synthesis of $\text{Li}_2\text{CoPO}_4\text{F}$ by mixing LiCoPO_4 from the first step with LiF in the appropriate stoichiometric ratio and then heating the mixture at 700 °C for 1.5 h in an argon atmosphere. Surface coating of the appropriate mass percentage (5 wt%) over $\text{Li}_2\text{CoPO}_4\text{F}$ was performed by the wet processing method as described in our earlier report.²⁷ A final heat treatment at 500 °C was necessary for removal of unwanted moieties and proper formation of the coating layer.

Structural confirmation of the synthesized uncoated and ZrO_2 coated $\text{Li}_2\text{CoPO}_4\text{F}$ samples were analyzed using X-ray diffraction studies (XRD, Rint 1000, Rigaku, Japan). Field emission scanning electron microscope (FE-SEM, S-4700, Hitachi, Japan) equipped with EX-200 energy dispersive X-ray spectroscopy (EDX) was used for morphological and chemical analysis of the sample. Cyclic voltammetry (CV) and electrochemical impedance spectroscopy (EIS) studies were carried out using an electrochemical work station (SP-150, Biologic, France) at room temperature. The EIS spectra were measured in the frequency range of between 100 kHz and 100 mHz using an applied current amplitude of 100 μA , while the CV was tested at a scan rate of 0.1 mV s^{-1} between the operating voltage of 2 V and 5.1 V with lithium being both a counter and reference electrode. Galvanostatic charge/discharge with a battery tester (WBCS 3000, Won-A-Tech, Korea) was used to evaluate the charge/discharge behavior of uncoated and ZrO_2 coated $\text{Li}_2\text{CoPO}_4\text{F}$ samples. The surface area of the synthesized powders was determined by Brunauer–Emmett–Teller (BET) the adsorption method using a surface area analyzer (ASAP 2020, Micromeritics Ins, USA).

The stability of the coating layer was tested by aging the sample at room temperature (25 °C) and at high temperature (50 °C) for a period of 30 days. The entire process was carried out in an Argon filled glove box that was maintained in an ultrahigh moisture controlled atmosphere and hence the influence of moisture from the external source was ruled out. Electrochemical characterizations of all the synthesized materials were performed using a CR2032

coin cell. The cell consisted of a synthesized material as a cathode and a metallic lithium anode separated by a polypropylene separator with 1 M LiPF_6 as an electrolyte. The cathodes were prepared with 20 mg of active material, 3 mg of Ketzen black (KB), and 3 mg of teflonized acetylene black (TAB) over a stainless steel current collector, followed by drying at 160 °C for 4 hrs before being used in the cell. Two sets of cells were prepared simultaneously, one for room temperature and the other for high temperature aging process. The assembled cells were carefully placed in a temperature chamber and were left undisturbed for 30 days. Electrochemical tests including CV and EIS were performed before and after aging and the effect of ZrO_2 coating in preserving the electrochemical activity of $\text{Li}_2\text{CoPO}_4\text{F}$ were analyzed extensively.

3. RESULTS AND DISCUSSION

The synthesized powders with and without ZrO_2 coating were weighted approximately in a glass vial and then heat treated at 120 °C overnight to remove the moisture absorbed during initial storage. About 5 ml commercial electrolyte, 1 M LiPF_6 in EC: DMC (1:1) was added to the heat treated sample under a controlled environment such that moisture from the external atmosphere does not affect the sample. The vial was shaken well before being left untouched for the aging process in two different temperature chambers (25 °C and 50 °C) for 30 days. The electrolyte solution was considered to be corrosive to the transition metal ions presented in the electrode active material, since even the high purity organic solvents would have a trace amount of water and could cause surface or bulk changes in the active mass.^{29,30} The amount of cobalt dissolution obtained using ICP for the coated sample was found to be 1/8th of that observed for the uncoated sample. The ratio of the sample weight to electrolyte volume was very high when compared with the practical situation, but this would ensure a proper distinction between the sample, the electrolyte, and the effect of temperature on metal dissolution. Metal dissolution can be due to the presence of H_3O^+ ion and the subsequent formation of acidic HF.²⁹ The high ratio of sample weight to electrolyte volume could be compared to the continuous reaction of metal with the anode in the practical batteries. In this situation, the quick metal ion saturation achieved in the electrolyte from the cathode reaction with the acidic species in the electrolyte, due to the small amount of electrolyte, would be compensated by the continuous removal of metal ions for reaction at the anode side. This circumstance can be clearly achieved in the glass vial with high electrolyte ratio through metal ion dissipation and hence the obtained data was considered to be valid. The reaction of the sample with electrolyte in the highly corrosive environment (50 °C) implied that there must be bulk changes in the sample.

The phase obtained for as-prepared and ZrO_2 coated LCPF samples were confirmed by XRD analysis and the

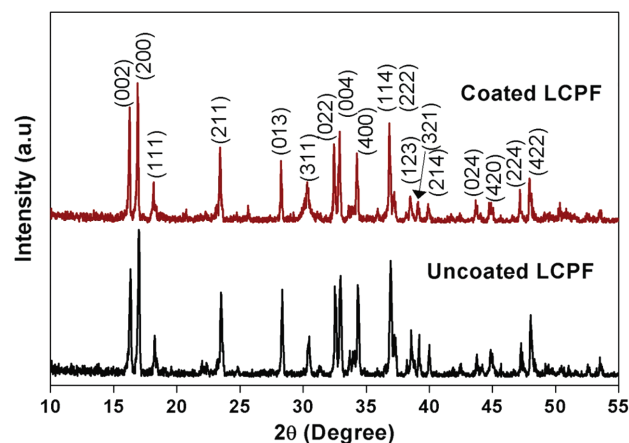


Figure 1. Powder XRD patterns of uncoated and 5 wt% ZrO_2 coated $\text{Li}_2\text{CoPO}_4\text{F}$ cathode materials.

results are shown in Figure 1. The XRD profiles of both uncoated and ZrO_2 coated LCPF did not show any impurity peaks such as LiCoPO_4 , LiF , CoP_3 , and Li_3PO_4 . At high temperatures, ZrO_2 could form a crystalline cubic phase, but the temperature handled after the coating process was about 500 °C, which was insufficient for transforming ZrO_2 into a crystalline phase. The non-availability of crystalline peaks of ZrO_2 in the XRD pattern proved that the coating layer was amorphous in nature. Also, the ZrO_2 was capable of withstanding temperatures as high as 500 °C. It is worth noting that the LCPF with coating neither transformed nor decomposed to the parent phase, similarly to LiCoPO_4 and LiF , during heat treatment after coating. On the other hand, no reflections pertaining to compounds containing oxides of lithium and zirconium were observed, which might have formed due to the penetration of Zr ions to the interior layer of crystalline LCPF during heat treatment. The 3D framework unit with highly stable PO_4 tetrahedral units meant that LCPF was less susceptible to phase transition during heat treatment with the coating substance; this differed to LiCoO_2 , where phase transition was evidenced by several previous reports.^{23,25,26} Furthermore, the reduction of phase transition during electrochemical cycling with the presence of ZrO_2 coating was considered to be the major reason for improved performance such as cycle stability, high rate stability, and improved Coulombic efficiency.

The morphological characteristics of the as prepared samples showed that the primary particles were in the order of 30~70 nm in size with strong agglomeration resulting in micrometer sized particles. In order to obtain a uniform coating over all particles, the sample was sonicated before being coated with ZrO_2 precursor. The sonication would separate the particles to some extent and could also prepare the surface of the particles for high adhesion. Later, during heat treatment after coating, the particles aggregated to form larger units. This process is clearly seen from the SEM pictures represented in Figure 2. The distribution of various elements in the ZrO_2 coated LCPF sample was

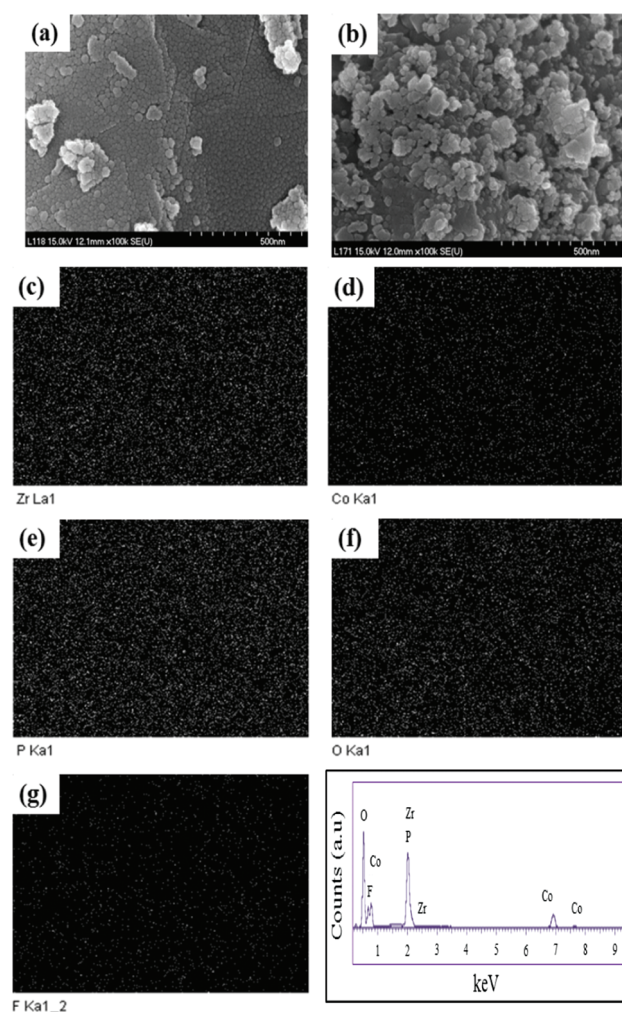


Figure 2. SEM images of (a) uncoated and (b) 5% ZrO_2 coated $\text{Li}_2\text{CoPO}_4\text{F}$ sample. Elemental mapping of (c) Zr, (d) Co, (e) P, (f) O and (g) F spectral signals of coated $\text{Li}_2\text{CoPO}_4\text{F}$ sample. The last picture elucidated elemental composition of ZrO_2 coated $\text{Li}_2\text{CoPO}_4\text{F}$ sample using EDX.

analyzed using the elemental mapping from SEM-EDX. The element mapping revealed a uniform distribution of the constituent elements of LCPF, i.e., Co, P, O, and F in the respective Figures 2(d)–(g). The existence and distribution of the most important candidate, zirconium, could be clearly seen from the Zr $K\alpha$ mapping represented in Figure 2(c). It was apparent from the strong Zr signals that the coating layer was homogeneously distributed over the LCPF particles. EDX also confirmed the elemental composition as shown in Figure 2. About 3 atomic percentages of zirconium ions was detected within the measured area with a calculated Co/F atomic ratio of 1. An increase in BET surface area from $2.54 \text{ m}^2 \text{ g}^{-1}$ for the uncoated sample to $3.05 \text{ m}^2 \text{ g}^{-1}$ for the coated LCPF was observed, which agreed with the BET surface area of additional oxides used for covering the LCPF particles.

The electrochemical performance of uncoated and 5% ZrO_2 coated LCPF samples was analyzed using various

techniques including cyclic voltammetry, impedance spectroscopy, and charge discharge studies using the as-prepared material in commercial electrolyte. The increased stability upon cycling for LCPF with ZrO_2 coating was evident from the uniform area under the curve within the initial few cycles, while the pristine LCPF had a continuous decreasing area with increase in cycle as seen in Figure 3. It was seen that the lithium intercalation and extraction in both uncoated and coated samples had a single broad peak during anodic and cathodic scans. The broad peak observed in the potential range of 3.0–3.5 V in the case of uncoated sample may be ascribed to the partial insertion of Li in the crystal lattice. This insertion can be due to the presence of CoF_2 impurity in the crystals, which is undistinguishable in the XRD pattern.³⁴ The subsequent cycles in the case of uncoated LCPF eventually followed a similar trend and more electrolyte decomposition would have led to a high acidic environment inside the cell. The acidic atmosphere was created by the formation of HF with the presence of a trace amount of moisture or H_3O^+ ions in the electrolyte combined with the increased temperature during the operation of battery. This would accelerate the transition metal to dissolve into the electrolyte and hence the continuous degrading of capacity for the uncoated cell.

High voltage cathode materials had a tendency for a high degree of electrolyte decomposition in the initial charging cycle. This resulted in decreased ability of the material to deliver high capacity. A balance needed to be made between the operating voltage and stability of the electrolyte; while both of these were crucial in the operation of high voltage cathode materials, none of these parameters can be compensated. Surface coatings have been demonstrated as a promising approach to protect the electro-active material and operation of the battery at high voltages.²⁵ The simultaneous lithium extraction and electrolyte decomposition restricted the appearance of proper peaks during the oxidation cycle in the case of the uncoated sample, while the coated sample delivered a peak at 5.0 V corresponding to the change in the valence state of cobalt ion. The disappearance of CV peaks in the uncoated sample could also be attributed to the metal dissolution that would have started simultaneously. It is worth noting that the current response due to electrolyte oxidation was limited in the coated sample, even during the initial cycle and was less than that observed in the uncoated sample. It was believed that a broad peak found for the pristine sample during the cathodic scan was due to lithium insertion at different structural sites, while this was not found in the coated sample. This could be due to the structural transformation occurring in the case of the uncoated sample during the initial cycle, which would create an empty site for lithium insertion due to cobalt dissolution. A more detailed study using highly sensitive *in-situ* X-ray diffraction studies is needed to confirm this assumption. Nevertheless, the cathodic insertion peak for the coated sample had higher current response

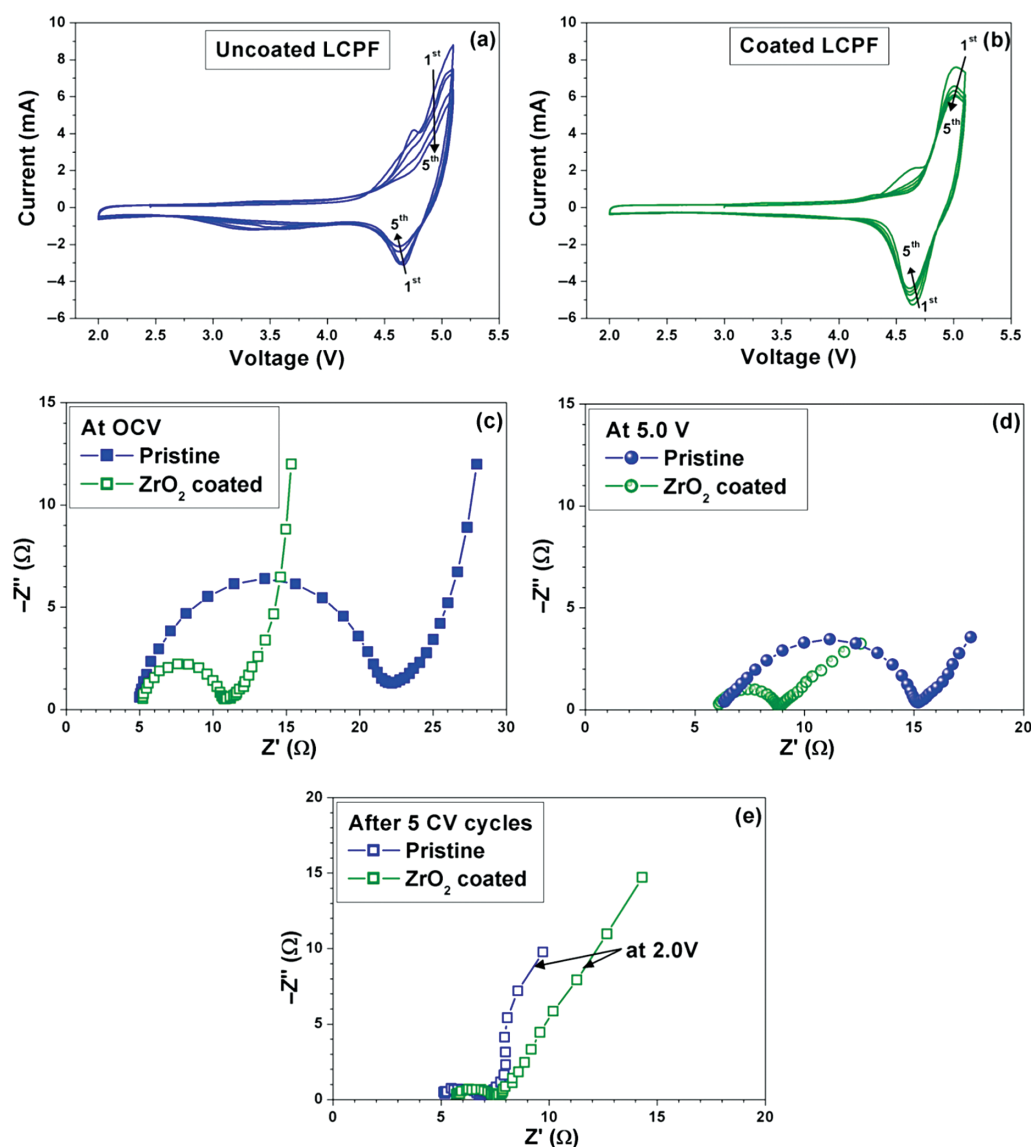


Figure 3. The initial 5 cycles of (a) uncoated and (b) coated $\text{Li}_2\text{CoPO}_4\text{F}$ materials obtained using cyclic voltammetry. Comparative electrochemical impedance studies of both uncoated and coated $\text{Li}_2\text{CoPO}_4\text{F}$ samples at (c) OCV, (d) charged state, i.e., at 5.0 V and (e) at discharged state (2.0 V). All data was collected from as-prepared cells without aging.

than that of the uncoated sample and dominated the electrochemical performance by a few orders.

The ZrO_2 surface coatings insulated the LCPF particles from each other, hence it was thought that a larger polarization would be encountered and this would effectively increase the resistance during electrochemical testing. The impedance results disproved this assumption immediately with a notable lower resistance for the coated sample than that of the uncoated LCPF. Impedance spectroscopy was carried out for as prepared cells of the coated and uncoated samples at an open circuit voltage (OCV) and then at a fully charged and discharge state; the results are shown in Figures 3(c)–(e). An average OCV of ~ 3.0 V versus Li^+/Li was recorded for all the cells. The impedance spectrum had a semicircle at the high frequency region and an inclined

line at the low frequency region. All cells had an almost similar solution resistance that validated the assembly and consistency of the cells. The absence of a separate semicircle for the surface coating at the high frequency region can be attributed to the thin surface coating over the LCPF particle and hence had not affected the overall resistance of the cell. The charge transfer resistance (R_{ct}) of the samples was calculated from the difference between the resistance obtained from the intersection of the semicircle at the high-medium frequency region and that at the high frequency region. A calculated R_{ct} of $22\ \Omega$ was obtained for the uncoated sample from Figure 3(c), while the 5% ZrO_2 coated sample had half the resistance ($11\ \Omega$). The introduction of an electronically insulating thin layer of coating does not increase the resistance; in contrast, a reduction

in overall resistance at OCV was observed. The resistance observed at the charged state of the cell (Fig. 3(d)) was found to decrease in the case of LCPF cathode materials. When the impedance was measured at the discharged state (Fig. 3(e)), the resistance was found to decrease to an even lower value. Interestingly, the resistance of the coated sample was less than that of the uncoated sample, even in the charged state at 5.0 V, while the resistance reaches almost the same value after the first discharge cycle (about 8 Ω for both cells). It could be demonstrated that the interface resistance can be reduced only after the first lithiation cycle. The inclined line denoted the solid state diffusion of Li^+ ions in the electrode. The variation in the degree of inclination for the coated and uncoated samples might be the result of significant heterogeneity in the composition within the framework LCPF particles.

A bulk change in the electrode active material was confirmed for electrodes after aging in various corrosive environments. FTIR, Raman, and XPS spectra obtained for the LiFePO_4 cathode materials after aging in commercial 1 M LiPF_6 electrolyte could be related to the formation of LiF , Li_xPF_x , and LiPOF_x with additional phases, and thus provided proof of electrolyte decomposition products formed even under undisturbed cell storage.³¹ The formation of an insulating film of LiF over the LCPF surface should have mitigated Li ion transport in and out of the particle during intercalation reaction. In this context, the 5% ZrO_2 coated LCPF sample was subjected to aging analysis. Cells made of the coated sample were assembled in an argon filled glove box and then left unattended at 25 $^\circ\text{C}$ and 50 $^\circ\text{C}$ in a precisely controlled temperature chamber for 30 days. The uncoated sample demonstrated degradation even under normal operating conditions (Fig. 4(a)), evidenced from the decreasing area of CV curves, and hence aging analysis was not performed on the uncoated samples. After aging under corrosive conditions, the cells with the coated sample were validated for electrochemical activity by CV and EIS. It was noticed that there was a slight increase in OCV for the cells after aging, to about 3.02 V for cells aged at 25 $^\circ\text{C}$ and 3.17 V for cells aged at 50 $^\circ\text{C}$. The increase in OCV was related to the development of SEI film at the negative electrode and the additional contribution of mobile lithium ions for the formation of SEI during storage.³² This effect was clearly shown with an increase in the overall resistance for aged cells at both temperatures (Fig. 4(b)). The resistance almost doubled for aged cells when compared with the resistance obtained at OCV for as-prepared cells. On the other hand, it was interesting to note that the increased resistance for the cells aged at two different temperatures was almost the same, which suggested that the harsh corrosive environment remaining at 50 $^\circ\text{C}$ had not affected the coated particle and might also have hindered the formation of LiF film from the reaction between the solvent molecules in the electrolyte and cathode active material. The electrochemical viability of the aged cells from both temperatures was tested by cyclic voltammetry between 2 V and 5.1 V.

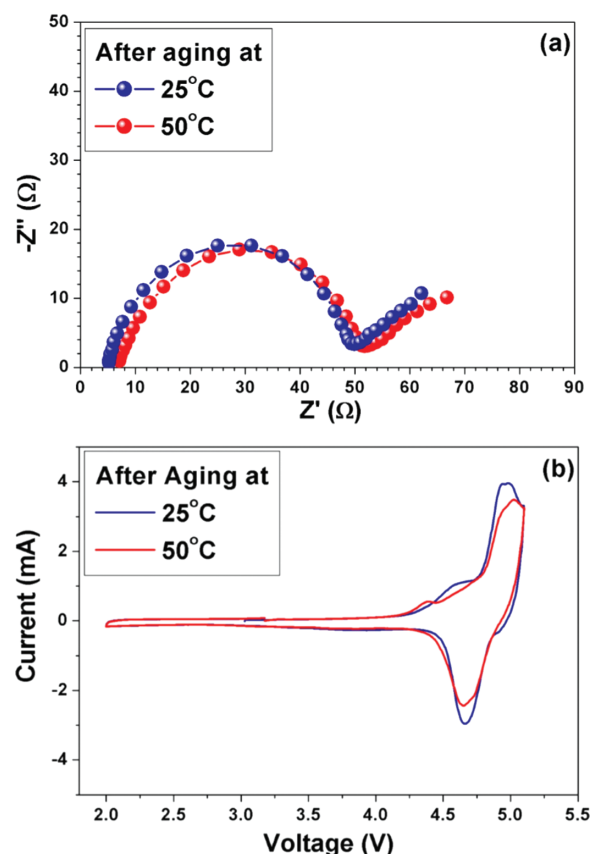


Figure 4. Electrochemical studies of coated $\text{Li}_2\text{CoPO}_4\text{F}$ cells aged in different temperatures. (a) Impedance at OCV immediately after storage and (b) the initial cycle recorded using cyclic voltammetry.

The current response obtained was impressive, exhibiting a similar profile to that observed for the as-prepared cells shown in Figure 3(b). All peaks resembled the same as those of as-prepared cells, which suggested that the storage did not alter the bulk properties of the cathode material and the ZrO_2 coating had obviously helped in protecting the LCPF particles. The anodic and cathodic peaks demonstrated fast kinetics of the aged cells, although there was a slight lag for the sample aged at 50 $^\circ\text{C}$. As expected, the cells aged at 50 $^\circ\text{C}$ displayed less capacity due to the highly corrosive environment withheld during aging.

The lithium extraction/insertion properties of both uncoated and coated LCPF were evaluated at various current rates and the results are presented in Figure 5. The cells were charged and discharged at 25, 50, 100, and 200 mA g^{-1} current rates at room temperature with three cycles in each rate and the results are shown in Figure 5(a). The uncoated sample showed a visible decrease in capacity upon cycling even at a slow rate with a maximum capacity of 109 mA h g^{-1} at a 25 mA g^{-1} current rate, while the coated sample maintained a similar capacity but with improved capacity retention. In terms of the rate performance of the cells, the coated sample exhibited considerably higher capacities in all current rates owing

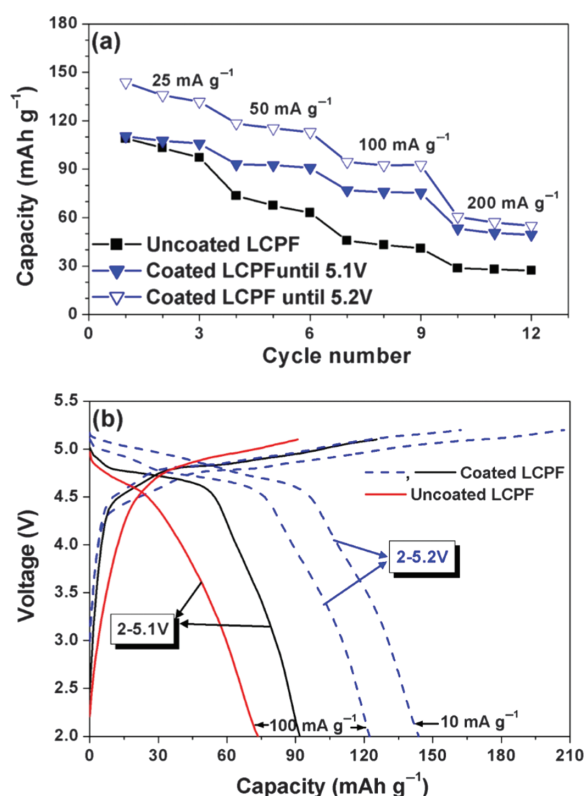


Figure 5. (a) Rate performance at various current rates of uncoated and coated $\text{Li}_2\text{CoPO}_4\text{F}$ cells. (b) Charge/discharge studies of uncoated and coated $\text{Li}_2\text{CoPO}_4\text{F}$ cells at different current rates and voltage ranges. The continuous line represents cells cycled at 2–5.1 V and the dotted line represent the voltage range 2–5.2 V.

to the protective nature of the coating. The durability of coating at a higher potential, i.e., 5.2 V, was tested at all the current rates specified including an additional rate (10 mA g^{-1}). A maximum capacity of 144 mA h g^{-1} was obtained for the coated sample which was charged up to 5.2 V. This result is considered as the highest capacity obtained for LCPF cathode material, considering the voltage limits used. The high rate capacity for cells cycled until 5.2 V was severely affected by the high electrolyte decomposition. In contrast, the discharge profile for the coated sample exhibited a clearer plateau region than that of the corresponding uncoated sample. In Figure 5(b), the charge-discharge curves of both samples are compared at the 100 mA g^{-1} current rate. A discharge capacity of 92 mA h g^{-1} was obtained for the coated sample, while the uncoated LCPF retained about a 20% lower capacity of 73 mA h g^{-1} . An irreversible capacity was observed for all the cells which are due to the presence of electrolyte decomposition at higher voltages. As a bi-functional oxide,³³ ZrO_2 adjusted to the prevailing environment and also helped the inner LCPF particles to avoid being directly in contact with the acidic species and thereby improved the electrochemical performance of the cathode active material.

4. CONCLUSION

The durability of ZrO_2 coating in enhancing the performance of $\text{Li}_2\text{CoPO}_4\text{F}$ was analyzed by aging the sample at two different temperatures. The powders aged in excess of the solvent were analyzed for cobalt dissolution and it was found that the ZrO_2 coated sample had less metal dissolution than the parent $\text{Li}_2\text{CoPO}_4\text{F}$. The cyclic voltammetry of aged cells showed dedicated peaks during anodic and cathodic scans, similar to those observed for as-prepared cells. The thin amorphous coating provided an area for electrolyte penetration but controlled the electrolyte oxidation through the bi-functional nature of the oxide. Nevertheless, the mechanical stability of the ZrO_2 coating withstood the high temperature and harsh corrosive environment within the battery and the heavy stress developed due to volume expansion facilitated the additional recovery of lithium during cycling and thus augmented the electrochemical performance of $\text{Li}_2\text{CoPO}_4\text{F}$.

Acknowledgments: This work was supported by the National Research Foundation of Korea Grant funded by the Korean Government (MEST) (NRF-2011-C1AAA001-0030538). Also, the work at BNL was supported by the U.S. Department of Energy, the Assistant Secretary for Energy Efficiency and Renewable Energy, Office of Vehicle Technologies under Contract Number DE-AC02-98CH10886.

References and Notes

1. M. Guilmard, C. Poullier, L. Croguennec, and C. Delmas, *Solid State Ionics* 160, 39 (2003).
2. Y. S. Lee, S. J. Cho, Y. K. Sun, K. Kobayakawa, and Y. Sato, *Electrochemistry* 73, 874 (2005).
3. Y. S. Lee, C. S. Yoon, Y. K. Sun, K. Kobayakawa, and Y. Sato, *Electrochem. Commun.* 4, 727 (2002).
4. Y. S. Lee and M. Yoshio, *Electrochem. Solid. St.* 4, A166 (2001).
5. K. Mizushima, P. C. Jones, P. J. Wiseman, and J. B. Goodenough, *Mater. Res. Bull.* 15, 783 (1980).
6. T. Ohzuku and Y. Makimura, *Chem. Lett.* 30, 642 (2001).
7. M. M. Thackeray, C. S. Johnson, J. T. Vaughan, N. Li, and S. A. Hackney, *J. Mater. Chem.* 15, 2257 (2005).
8. M. M. Thackeray, W. I. F. David, P. G. Bruce, and J. B. Goodenough, *Mater. Res. Bull.* 18, 461 (1983).
9. A. K. Padhi, K. S. Nanjundaswamy, and J. B. Goodenough, *J. Electrochem. Soc.* 144, 1188 (1997).
10. V. Aravindan, K. Karthikeyan, K. S. Kang, W. S. Yoon, W. S. Kim, and Y. S. Lee, *J. Mater. Chem.* 21, 2470 (2011).
11. K. Karthikeyan, V. Aravindan, S. B. Lee, I. C. Jang, H. H. Lim, G. J. Park, M. Yoshio, and Y. S. Lee, *J. Power Sources* 195, 3761 (2010).
12. K. Karthikeyan, V. Aravindan, S. B. Lee, I. C. Jang, H. H. Lim, G. J. Park, M. Yoshio, and Y. S. Lee, *J. Alloys Compd.* 504, 224 (2010).
13. V. Aravindan, J. Gnanaraj, Y. S. Lee, and S. Madhavi, *J. Mater. Chem. A* 1, 3518 (2013).
14. C. Masquelier and L. Croguennec, *Chem. Rev.* 113, 6552 (2013).
15. A. K. Padhi, K. S. Nanjundaswamy, C. Masquelier, S. Okada, and J. B. Goodenough, *J. Electrochem. Soc.* 144, 1609 (1997).
16. M. Dutreilh, C. Chevalier, M. El-Ghozzi, D. Avignant, and J. M. Montel, *J. Solid State Electr.* 142, 1 (1999).

17. J. M. Le Meins, M. P. Crosnier-Lopez, A. Hemon-Ribaud, and G. Courbion, *J. Solid State Chem.* 148, 260 (1999).
18. O. V. Yakubovich, O. V. Karimov, and O. K. Mel'nikov, *Acta Crystallogr. C* 53, 395 (1997).
19. S. C. Yin, P. S. Herle, A. Higgins, N. J. Taylor, Y. Makimura, and L. F. Nazar, *Chem. Mater.* 18, 1745 (2006).
20. J. Hadermann, A. M. Abakumov, S. Turner, Z. Hafideddine, N. R. Khasanova, E. V. Antipov, and G. Van Tendeloo, *Chem. Mater.* 23, 3540 (2011).
21. N. R. Khasanova, A. N. Gavrilov, E. V. Antipov, K. G. Bramnik, and H. Hibst, *J. Power Sources* 196, 355 (2011).
22. S. Okada, M. Ueno, Y. Uebou, and J.-I. Yamaki, *J. Power Sources* 146, 565 (2005).
23. Y. J. Kim, J. Cho, T.-J. Kim, and B. Park, *J. Electrochem. Soc.* 150, A1723 (2003).
24. Z. Chen and J. R. Dahn, *Electrochem. Solid St.* 5, A213 (2002).
25. J. Cho, Y. J. Kim, T.-J. Kim, and B. Park, *Angew. Chem. Int. Edit.* 40, 3367 (2001).
26. L. Liu, L. Chen, X. Huang, X.-Q. Yang, W.-S. Yoon, H. S. Lee, and J. McBreen, *J. Electrochem. Soc.* 151, A1344 (2004).
27. S. Amaresh, K. Karthikeyan, K. J. Kim, M. C. Kim, K. Y. Chung, B. W. Cho, and Y. S. Lee, *J. Power Sources* 244, 395 (2013).
28. S. Amaresh, G. J. Kim, K. Karthikeyan, V. Aravindan, K. Y. Chung, B. W. Cho, and Y. S. Lee, *Phys. Chem. Chem. Phys.* 14, 11904 (2012).
29. T. Kawamura, S. Okada, and J.-I. Yamaki, *J. Power Sources* 156, 547 (2006).
30. R. Oesten, U. Heider, and M. Schmidt, *Solid State Ionics* 148, 391 (2002).
31. M. Koltypin, D. Aurbach, L. Nazar, and B. Ellis, *J. Power Sources* 174, 1241 (2007).
32. M. Koltypin, D. Aurbach, L. Nazar, and B. Ellis, *Electrochem. Solid St.* 10, A40 (2007).
33. X. Bo-Qing, Y. Tsutomu, and T. Kozo, *Chem. Lett.* 17, 1663 (1988).
34. W. K. Behl and J. A. Read, *ECS Trans.* 41, 97 (2012).

Received: 16 September 2013. Accepted: 20 October 2013.

Delivered by Publishing Technology to: Sung Kyun Kwan University
IP: 115.145.198.168 On: Tue, 13 May 2014 01:58:38
Copyright: American Scientific Publishers